SPACE TELESCOPE SCIENCE INSTITUTE
Operated for NASA by AURA

Instrument Science Report ACS 2004-016

ACS coronagraphic flat fields

J. Krist, J. Mack, & R. Bohlin
August 30, 2004

ABSTRACT

Due to vignetting by the Lyot stop and the presence of occulting spots, ACS coronagraphic flat fields are different than those used for calibrating normal ACS/HRC images. An additional complication is caused by the random, time-dependent motions of the occulting spots. Flat fielding of an ACS coronagraphic image requires division by a pixel-to-pixel flat followed by division of a separate flat that contains the vignetting patterns of the occulting spots, appropriately shifted to match their locations for a particular observation date. Coronagraphic flats can only be obtained on-orbit for a few filters, so some must be derived from prelaunch calibration data. Given the limited number of datasets available from which to construct flats and the fact that ACS coronagraphic programs are dominated by imaging of extended sources (circumstellar disks), the correction of throughput variations to <2% on spatial scales of a few pixels or more is the goal.

Introduction

The ACS/HRC coronagraph allows high contrast imaging of faint sources (disks, galaxies) near bright objects (stars, quasar nuclei). The coronagraph consists of two occulting spots, 0.9” and 1.5” in radius, and a Lyot stop that suppress diffracted light from the telescope. Both the spots and Lyot stop are mounted on a panel attached to the calibration door mechanism so that they can be moved into the beam as needed and removed when normal imaging takes place. They alter, compared to the normal imaging mode, the effective response pattern over the field that is typically removed via flat fielding.

The Lyot stop, which is a mask that looks like an exaggerated version of the telescope's obscuration pattern, creates large-spatial-scale variations in throughput over the field and also modifies the diffraction patterns caused by dust on the optics.

The occulting spots, which are located in the aberrated beam, have extended vignetting patterns caused by the large size of the uncorrected PSF. A spot's intensity pattern appears as the convolution of the aberrated PSF with a dark circle. For the r=0.9" spot, the vignetting pattern can extend out to r=2", with a 20% reduction in throughput at 0.25" beyond the spot's edge. Because of the variation in the PSF with wavelength, the spot patterns vary with filter. Additional complexity results from apparently random motions of the spots by up to 4 pixels over weekly timescales. The spot positions are measured about once a week using images of the Earth taken in filter F330W.

Because the masks are located on the calibration door mechanism, it is not possible to take internal coronagraphic flats. Earth flats can only be obtained in the shortest and longest wavelength filters (up to F475W on the short end and in the ramp filters on the long), otherwise saturation occurs with the shortest exposure time. The only coronagraphic flats available for most of the filters are from pre-flight calibration images. In these the spots are located tens of pixels from their current mean positions due to gravity release effects that occurred after launch. Thus, there are no flat fields that can be applied as-is to accurately calibrate the on-orbit coronagraphic data.

Any flats must be cobbled together from a combination of pre-launch laboratory and on-orbit images. Pre-launch lab or (when available) earth flats can be used to derive the pixel-to-pixel (*P-flat*) and low-spatial-frequency (*L-flat*) variations, as well as the occulting spot vignetting patterns. Regions in those images affected by the spots can be replaced by the corresponding pixels from the noncoronagraphic LP flats derived from on-orbit data to produce spot-less coronagraphic flats (*low-order-and-pixel-to-pixel* or *LP-flats*). A flat containing only the occulting spot patterns (*spot flats*) can then be shifted as necessary for each observation to account for time-dependent motions and then divided out separately after dividing by the LP-flat.

The creation of the coronagraphic LP and spot flats is an involved process using data from disparate sources, and so they have been generated for only a few select filters, namely F330W, F435W, F475W, F606W, and F814W.

Initial Analysis of the Coronagraphic Flat Field Pattern

To verify the throughput variations over the coronagraphic field on-orbit, images were taken of a roughly uniform region of the Orion Nebula (Figure 1) through F606W with and without the coronagraph (program 9016). The calibrated, noncoronagraphic image represents the “truth”. Division of the uncalibrated coronagraphic exposure by this truth image (after appropriate registration) provides the coronagraphic flat field response for F606W, though at low signal-to-noise (Figure 2).

Figure 2 also shows the derived coronagraphic flat divided by an on-orbit noncoronagraphic flat. There is a 5% slope in the residual response variation that decreases from the upper left to lower right of the detector. This is quite similar to the L-flat correction applied to the pre-launch noncoronagraphic flats (no such correction is necessary for the pre-launch coronagraphic flats).

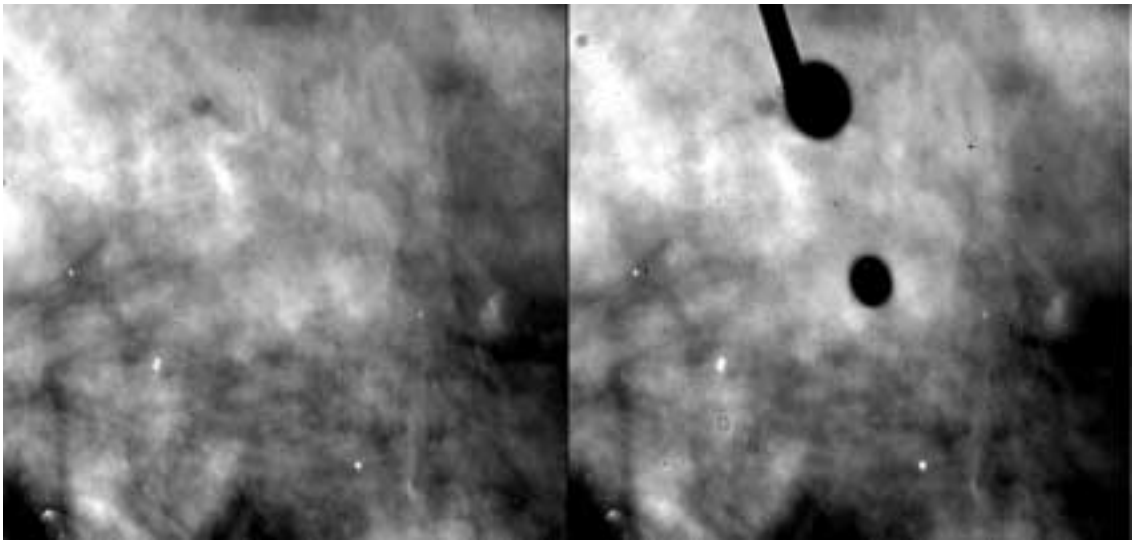

Figure 1: (Left) Noncoronagraphic HRC image of a region of the Orion Nebula after flat fielding. The frame is compose of dithered images, so the occulting finger has been filled in. (Right) HRC image of the same region taken with the coronagraph in place and with no flat fielding. Both images are displayed between 80% - 120% of the median image values.

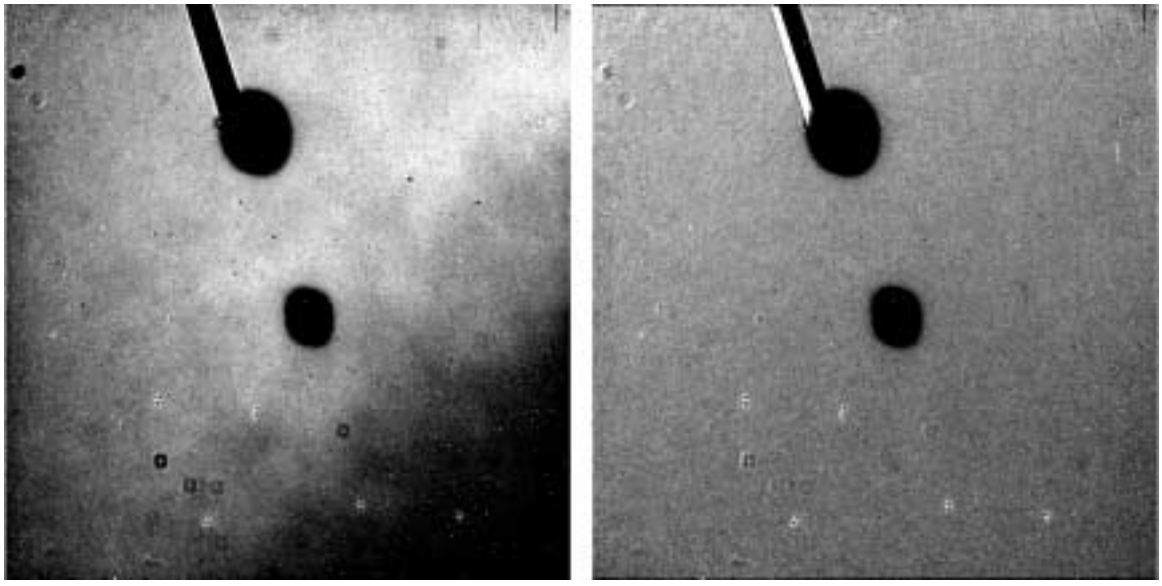

Figure 2: (Left) Result of dividing the non-flattened, coronagraphic image of the Orion Nebula by the flat-fielded, direct image of the same region. This reveals the effective response pattern of the coronagraph. The frame is displayed between 95% - 105% of the median image value. Stars from the Orion Nebula image are visible. (Right) Image on left divided by the noncoronagraphic flat field, displayed at the same scale. This shows that there is a 5% difference across the field between noncoronagraphic and coronagraphic flats.

The Flat Fielding Process

As of the time of writing, the ACS pipeline contains coronagraphic-specific LP-flats for the five filters listed above. For coronagraphic observations using the other filters, noncoronagraphic HRC flat fields are used that have neither the occulting spot patterns nor a correction for the 5% slope difference seen in Figure 2.. Calibrated data requested from the HST archive will be divided by these flats, providing correction for field and pixel-to-pixel variations (though with larger errors for those using the noncoronagraphic flats). Because of the differences between the non- and coronagraphic flats, the use of filters other than those that have coronagraph-specific flats is discouraged in the ACS Instrument Handbook.

The pipeline does not currently contain or use spot flats. The observer must therefore manually download the appropriate spot flat from the ACS Reference Files web page at:

http://www.stsci.edu/hst/acs/analysis/reference_files/hrc_coron_spotflat_list.html

That page also contains a table listing dates and corresponding offsets of the spot relative to its position in the spot flat. The observer must look up the appropriate offset for the date

nearest his/her science observation and then shift the spot flat by that amount. Bilinear interpolation suffices, such as that used in the *imshift* IRAF task (making sure that pixels shifted off the edge are replaced by 1.0). Because the two occulting spots are located on the same glass substrate, they shift by the same amount. The science image can then be divided by the shifted spot flat. The division must be done on the distorted image (_flt or _crj) before geometric distortion correction.

By Fall 2004, the ACS pipeline will likely perform the task of shifting and dividing out the spot flats, eliminating the need for observers to manually process the data. However, because of the time lag in the weekly measurement of the spot positions and the time the shift table is updated, pipeline-calibrated data may not be optimal for images extracted from the archive shortly after the observations were made.

Because the flat fields are always normalized to a mean value of unity in the central region, the coronagraphic flats do not compensate for the fact that the throughput in the coronagraph is only 0.475 that in the normal imaging mode due to the Lyot stop.

Flat Field Creation

F330W, F435W, F475W

Earth flats have been taken through F330W, F435W, and F475W. F330W is used for weekly monitoring of the occulting spot position (program 9658 in Cycle 12 and 10050 in Cycle 13), so there are many earth flats available for it (Figure 3). As part of program 9658 a small number of coronagraphic earth flats were obtained through F435W, F475W, and a couple of narrowband filters.

Because of streaks introduced by clouds and other Earth features, care must be taken to select earth flats that are as free of such structures as possible while having sufficient signal-to-noise to provide reasonable pixel-to-pixel calibration accuracies. In each filter a median flat was first obtained using visually-selected, median-normalized images that had minimal streaking and mean intensities above a specified level. Then each flat was divided by this median flat and either rejected or accepted based on the apparent amount of streaking. A new median flat was then created from the accepted frames and the procedure iterated again. In the end, 11 images were used for the final F330W flat, 5 for F435W, and 3 for F475W (the three F475W images were combined with cosmic ray rejection).

The occulting spot patterns in these final LP-flats were replaced with corresponding regions from the noncoronagraphic flats. For the small spot a r=2” region was replaced

while a *r*=2.9” one replaced the large spot. The edges of these regions were weighted to blend data smoothly between the final and noncoronagraphic flats. Differences in illumination slopes across these regions were accounted by adding a linearly sloping offset measured near their edges. The LP-flats, including those derived for other filters, are normalized so that they have a mean value of 1.0 in the region (x1:x2,y1:y2) = (460:563,460:563), as the noncoronagraphic flats are.

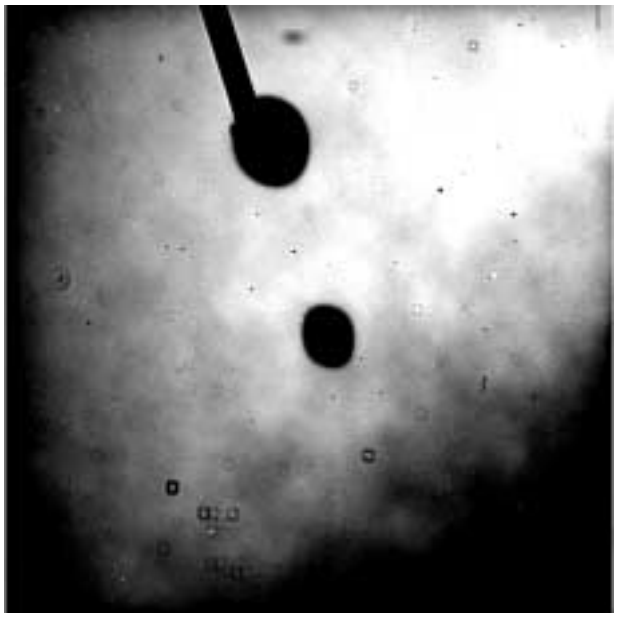

Figure 3: Earth flat taken through F330W, displayed between 95% - 105% of the median image value.

The occulting spot flats for these filters were derived from one or two combined earth flats after division by the LP-flat. The same-sized regions used to remove the spots from the LP-flat were used to extract them from these flattened earth flats. Because the occulting finger covers the left side of the large spot, the subimage of that spot was rotated 180 degrees about the spot center. The region in the original spot flat affected by the finger was then replaced by the corresponding pixels in the rotated flat, producing a symmetrical spot image without the finger. The spot subimages were then placed in a 1K x 1K image in which all values outside of the spot regions were set to one. A 9-pixel diameter circular median filter was then applied to smooth out pixel-to-pixel noise. The spots were shifted so that the small spot is centered at (547,467) in (0,0) first-pixel coordinates (this centering is applied to all spot flats).

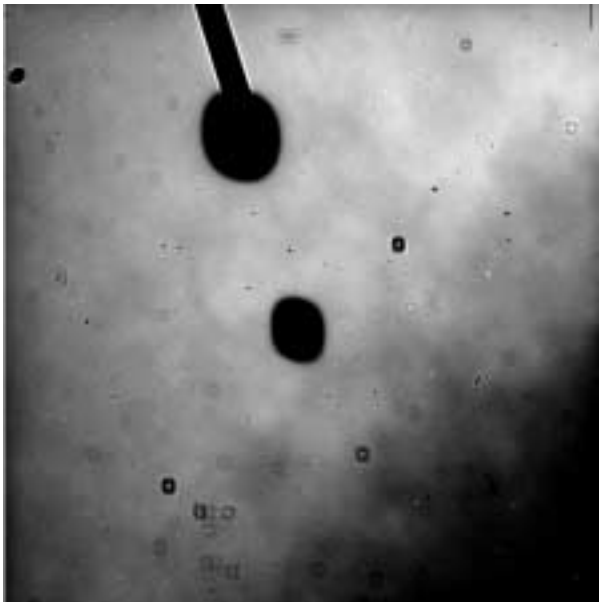

Figure 4: Prelaunch flat taken through F606W, displayed between 95% - 105% of the median image value.

F606W, F814W

Earth flats cannot be taken through F606W and F814W due to saturation, so modified versions of the prelaunch lab flats (Figure 4) must be used.

Comparison of the F606W prelaunch flat with the pattern derived from the Orion Nebula data showed that the small, circular diffraction patterns (*rings*) created by defects in or dust on the ACS optics were offset between the two images while the other features remained stationary. This may be due to gravity-release shifts. The smaller, sharp, dark features (*specks*) caused by material located on the detector appeared stationary. The rings are about 30 pixels in diameter and vary the effective throughput by >10% over their area, so it was necessary to deal with their offsets to prevent obvious errors in images of extended objects like disks. Likewise, the specks, though small, vary throughput by as much as 90% and must also be preserved. The specks were identified in the noncoronagraphic HRC F606W and F814W flats using crude spatial filtering. The absolute difference between a normal flat and a 9 x 9 pixel median-smoothed version of itself was computed and all pixels whose difference values were beyond an empirically-derived limit were classified as specks. The prelaunch flats were shifted by two pixels to correctly register the rings, then the specks in the shifted image were filled in with pixels from the normal flats and new specks added at the proper locations. Also, a dust spot located in the prelaunch flats at (x,y)=(672,618) but not seen in the on-orbit flats was replaced by patching in pixels from the normal flats (Figure 5).

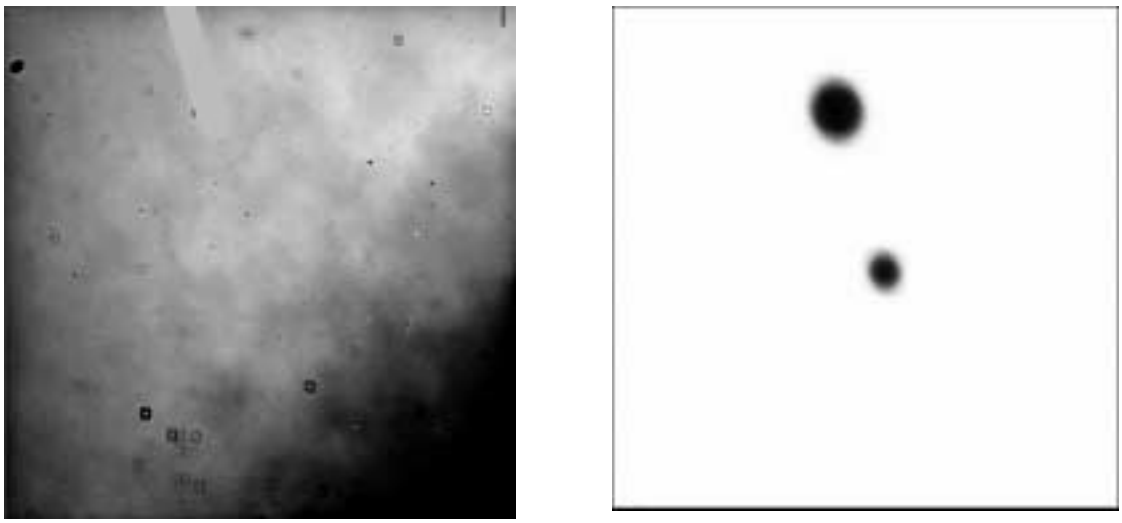

Figure 5: (Left) Coronagraphic P-flat for F606W derived from the prelaunch data. The spots have been replaced by regions patched in from the normal F606W flat. Displayed between 95%-105% of the median image value. (Right) Spot flat for F606W derived from the prelaunch flat and including the correction based on the residuals seen in the Orion Nebula-derived response pattern.

This process obviously has drawbacks. While preserving dust ring and speck features, and not significantly impacting lower spatial frequency structure, the shifting invalidates the pixel-to-pixel corrections that the flats make to the data. However, pixel-to-pixel differences between the shifted and unshifted flats are <1% for 90% of the pixels and <2% for >99% of the pixels, so this is not considered to be a significant problem.

The spot flats (Figure 5) were generated in the same manner as the earth flat-derived ones. As described below, dividing the Orion Nebula-derived response pattern by the new F606W LP-flat and spot flat resulted in some significant residuals around the spot perimeters. A correction was made to the spot flat based on a median-filtered version of these residuals. The residuals likely result from the difference in illumination between the prelaunch and on-orbit configurations.

Testing the F606W Flat

The response pattern derived from the Orion Nebula was divided by the new F606W LP-flat and the corresponding spot flat after registration of the spot pattern. The result (Figure 6) showed that the RMS variations on scales of larger than a few pixels (excluding the

spots) over the entire image were reduced from ~2% to ~0.6%. In the lower right corner of the detector, where the response is lower than average, the RMS variation is reduced from 4.5% to 0.4%. No correction appears to be required for differences in the low-spatial-scale variations between the prelaunch lab and on-orbit coronagraphic flats, unlike that required for noncoronagraphic flats. During the prelaunch calibrations the pupil and illumination patterns used for normal flats were not exactly like that produced by the telescope, so L-flat corrections are needed. However, because the Lyot stop defined the pupil pattern in the coronagraphic ground tests, as well as on-orbit, there is no need for such correction.

With the initial F606W spot flat there were bright, asymmetric residuals around both spots at the 4%-5% level (Figure 6). The small spot pattern was corrected as described in the previous section (Figure 7). The large spot pattern was not modified due to the combination of interference from the occulting finger and the residual asymmetry (the large spot is not used by any program, either). Similar errors may exist for the F814W spot flat, but there are no data in that filter that can be used to derive a correction.

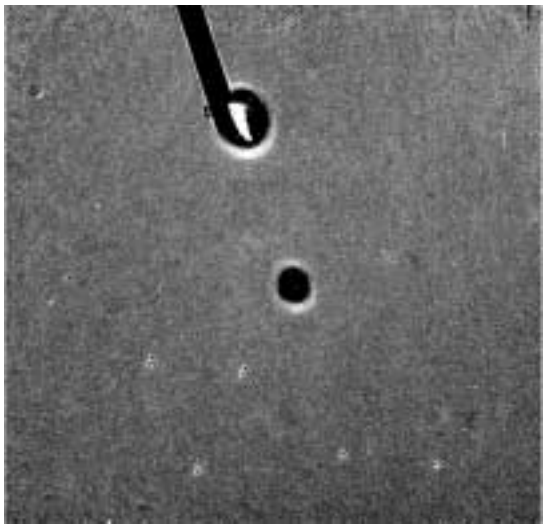

Figure 6: Orion Nebula-derived response pattern divided by the F606W coronagraphic LP-flat and the initial F606W spot flat. Differences between the on-orbit spot patterns and those in the prelaunch data result in the 4%-5% residuals seen around the spots. Displayed between 97%-105% of the median image value. Residuals caused by stars are visible.

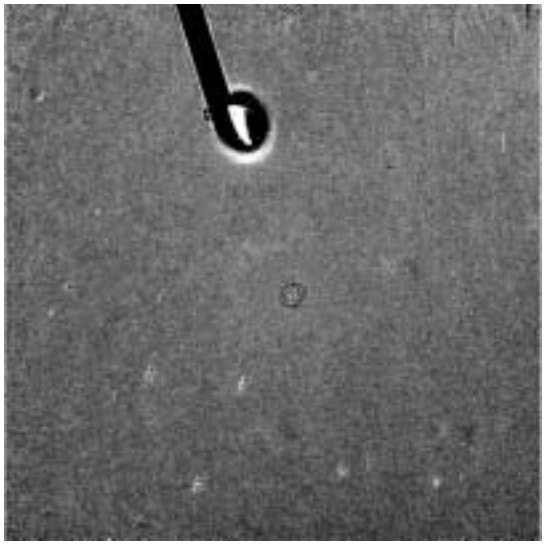

Figure 7: As in Figure 6, but divided by the modified spot. Displayed between 97%-105% of the median image value.

Spot Position Differences Between Filters

Comparisons of F330W, F435W, and F475W coronagraphic earth flats show that the occulting spot patterns appear at slightly different locations depending on the filter. Offsets of 0.5 pixel are seen. The shifts with filter seen on-orbit are not the same as those seen in the pre-launch lab data for unknown reasons.

The provided spot flats are all aligned to the same location, and the table of shifts relative to date is derived from F330W images and is exact only for F330W spot flats. Shifts applied to the spot flats for the other filters will result in a slight positional error. However, an error of 0.4 pixels results in only a 1% intensity error at the edge of the spot. In comparison, a positional error of 4 pixels creates a 40% intensity error.